Eur. J. Biochem. **267**, 566–572 (2000) © FEBS 2000

Contribution of disulfide bonds to the conformational stability and catalytic activity of ribonuclease A

Tony A. Klink[1], Kenneth J. Woycechowsky[1], Kimberly M. Taylor[2] and Ronald T. Raines[1,3]

[1]*Department of Biochemistry,* [2]*Graduate Program in Biophysics, and* [3]*Department of Chemistry, University of Wisconsin–Madison, WI, USA*

Disulfide bonds between the side chains of cysteine residues are the only common crosslinks in proteins. Bovine pancreatic ribonuclease A (RNase A) is a 124-residue enzyme that contains four interweaving disulfide bonds (Cys26–Cys84, Cys40–Cys95, Cys58–Cys110, and Cys65–Cys72) and catalyzes the cleavage of RNA. The contribution of each disulfide bond to the conformational stability and catalytic activity of RNase A has been determined by using variants in which each cystine is replaced independently with a pair of alanine residues. Thermal unfolding experiments monitored by ultraviolet spectroscopy and differential scanning calorimetry reveal that wild-type RNase A and each disulfide variant unfold in a two-state process and that each disulfide bond contributes substantially to conformational stability. The two terminal disulfide bonds in the amino-acid sequence (Cys26–Cys84 and Cys58–Cys110) enhance stability more than do the two embedded ones (Cys40–Cys95 and Cys65–Cys72). Removing either one of the terminal disulfide bonds liberates a similar number of residues and has a similar effect on conformational stability, decreasing the midpoint of the thermal transition by almost 40 °C. The disulfide variants catalyze the cleavage of poly(cytidylic acid) with values of k_{cat}/K_m that are 2- to 40-fold less than that of wild-type RNase A. The two embedded disulfide bonds, which are least important to conformational stability, are most important to catalytic activity. These embedded disulfide bonds likely contribute to the proper alignment of residues (such as Lys41 and Lys66) that are necessary for efficient catalysis of RNA cleavage.

Keywords: conformational stability; differential scanning calorimetry; disulfide bond; enzyme; ribonuclease A.

A polypeptide chain can adopt many conformations. Yet, the sequence of its amino-acid residues directs folding to a particular native state [1]. The loss of conformational entropy associated with folding destabilizes the native conformation. This destabilization is overcome by the hydrophobic effect, hydrogen bonds, other noncovalent interactions, and (for many proteins) disulfide bonds [2].

Bovine pancreatic ribonuclease A (RNase A; EC 3.1.27.5 [3,4]) provides a superb template with which to dissect the contribution of disulfide bonds to conformational stability. RNase A consists of 124 amino-acid residues and contains four intrachain disulfide bonds (Cys26–Cys84, Cys40–Cys95, Cys58–Cys110, and Cys65–Cys72; Fig. 1). The four disulfide bonds are conserved in all 40 of the known sequences of homologous mammalian pancreatic ribonucleases [5]. Two disulfide bonds (Cys40–Cys95 and Cys65–Cys72) link together surface loops, and two link an α-helix to a β-sheet in the protein core (Cys26–Cys84 and Cys58–Cys110). Three disulfide bonds enclose a loop of similar size (Cys26–Cys84, Cys40–Cys95 and Cys58–Cys110; $\eta = 59$, 56, and 53, respectively), and the other disulfide bond (Cys65–Cys72; $\eta = 8$) encloses a smaller loop.

In previous work, the cystines of RNase A were replaced with pairs of serine residues [6]. Drawing conclusions from this study is problematic because replacing a cystine with a pair of serine residues can result in an overestimation of the importance of disulfide bonds [7]. Cystine residues are nonpolar and are usually buried in folded proteins [8,9]. Indeed, the disulfide bonds of native RNase A have little or no solvent-accessible surface area (Fig. 1). In contrast, a serine side chain is polar and likely to be highly destabilizing in the hydrophobic environment of a protein core.

Here, we have used site-directed mutagenesis to replace each cystine in RNase A with a pair of alanine residues. The four disulfide variants are active catalysts of RNA cleavage. We assessed the contribution of disulfide bonds to the conformational stability of each variant by monitoring thermal unfolding using ultraviolet spectroscopy and differential scanning calorimetry (DSC). We find that the disulfide bonds that restrict the N- and C-termini (Cys26–Cys84 and Cys58–Cys110) are the most important to conformational stability. In constrast, the disulfide bonds proximal to active site residues (Cys65–Cys72 and Cys40–Cys95) are most important to catalytic activity.

Correspondence to R. T. Raines, Department of Biochemistry, University of Wisconsin–Madison, 433 Babcock Drive, Madison, WI 53706-1544, USA.
Fax: + 1608 2623453, Tel.: + 608 2628588,
E-mail: raines@biochem.wisc.edu

Abbreviations: BPTI, bovine pancreatic trypsin inhibitor; DSC, differential scanning calorimetry; poly(C), poly(cytidylic acid); RNase A, bovine pancreatic ribonuclease A.

Enzyme: ribonuclease (EC 3.1.27.5)

Note: web page available at http://www.biochem.wisc.edu/raines

(Received 22 September 1999, accepted 23 November 1999)

EXPERIMENTAL PROCEDURES

Escherichia coli strains DH11S and DH5α were from Gibco BRL. *E. coli* strain BL21(DE3) (F^- ompT r_B^- m_B^-) was from Novagen. *E. coli* strain CJ236 and helper phage M13K07 were from Bio-Rad. All enzymes for the

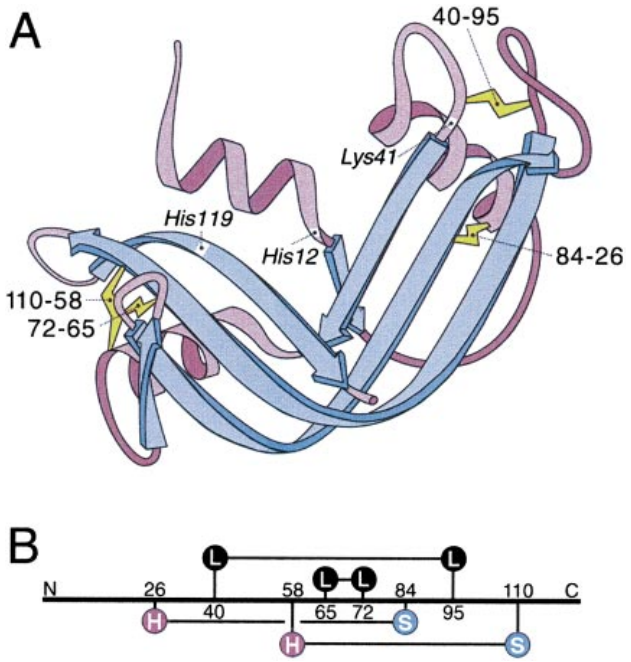

Fig. 1. Structural representations of ribonuclease A. (A) Ribbon diagram with inscriptions referring to the location of the disulfide bonds and active-site residues. The solvent-accessible surface area (0.52 nm^2 = 100%) of the cystine side chains in the crystalline protein (PDB entry 7RSA) are Cys26–Cys84, 0 nm^2; Cys58–Cys110, 0.02 nm^2; Cys40–Cys95, 0.06 nm^2; and Cys65–Cys72, 0.07 nm^2. (B) Scheme showing the connectivity of the disulfide bonds. The secondary structural context of the half-cystines is indicated by H, α-helix; L, surface loop; or S, β-sheet.

manipulation of recombinant DNA were from Promega or New England Biolabs. Purified oligonucleotides were obtained from Gibco BRL. DNA was sequenced with a Sequenase 2.0 kit from United States Biochemicals or with an ABI 373 Automated Sequencer using an ABI PRISM Dye Terminator Cycle Sequencing Ready Reaction Kit with AmpliTaq DNA Polymerase, FS (Foster City, CA, USA) and an MJ Research PTC-100 Programmable Thermal Controller (Watertown, MA, USA). FPLC Hiload 26/60 Superdex 75 gel filtration column and mono-S HR10/10 cation-exchange columns were from Pharmacia LKB. Poly(cytidylic acid) [poly(C)] was from Midland Certified Reagent (Midland, TX, USA) and was precipitated from ethanol and washed with aqueous ethanol (70% v/v) before use. IPTG was from Gold Biotechnology (St Louis, MO, USA). Bacto yeast extract, Bacto tryptone, Bacto peptone, and Bacto agar, were from Difco. LB medium contained (in 1.00 L) Bacto tryptone (10 g), Bacto yeast extract (5 g), and sodium chloride (10 g). TB Reagents medium contained (in 1.00 L) Bacto tryptone (12 g), Bacto yeast extract (24 g), glycerol (4 mL), KH_2PO_4 (2.31 g), and K_2HPO_4 (12.54 g). All media were prepared in distilled, deionized water and autoclaved. All other chemical reagents were of commercial reagent grade or better, and were used without further purification unless indicated otherwise. *E. coli* cell lysis was performed using a French pressure cell from SLM Aminco (Urbana, IL, USA). Ultraviolet and visible absorbance measurements were made with a Cary 3 double beam spectrophotometer equipped with a Cary temperature controller from Varian (Sugar Land, TX, USA). Calorimetry experiments were performed with an MCS differential scanning calorimeter (DSC) from MicroCal (Northampton, MA, USA).

Preparation of ribonuclease A variants

Oligonucleotide-mediated site-directed mutagenesis was used to create four RNase A variants in which a cystine was replaced with a pair of alanine residues. Plasmid pBXR directs the expression of RNase A in *E. coli* [10]. Mutagenesis was performed on plasmid pBXR replicated in *E. coli* strain DH11S or CJ236 [11]. To produce the DNA encoding C26A/C84A RNase A, the TGT codon for Cys26 in the wild-type plasmid pBXR was replaced with GCG (reverse complement in bold) using the oligonucleotide: AGGTTCCGGCTTTTCATCATCTGGTT**CGC**GTAGTTGGAGC, and the TGC codon for Cys84 was replaced with GCC (reverse complement in bold) using the oligonucleotide: CTGCCGGTCTCCCG**GGC**GTCGGTGATGC. DNA encoding C40A/C95A RNase A was produced by replacing the TGC codon for Cys40 with GCG (reverse complement in bold) using the oligonucleotide: GTTCACTGGCTT**CGC**TCGATCTTTGGT, and the TGT codon for Cys95 was replaced with GCG (reverse complement in bold) using the oligonucleotide: GGTCTTGTAGGC**CGC**GTTGGGGTACTT. DNA encoding C58A/C110A RNase A was produced by replacing the TGC codon for Cys58 with GCG (reverse complement in bold) using the oligonucleotide: TTCTGGGA**CGC**CACGGCCTGGACGTCAGCCAG, and the TGT codon for Cys110 was replaced with GCG (reverse complement in bold) using the oligonucleotide: GGCACGTATGGGTTTCCCTC**CGC**AGCCACAA. Replacing the TGC codons for Cys65 and Cys72 with GCG produced DNA encoding C65A/C72A RNase A (reverse complements in bold) using the oligonucleotide: CTCTGGTA**CGC**ATTGGTCTGCCCATTCTT**CGC**GGCAACAT. Mutagenesis reaction mixtures were transformed into competent DH5α cells, and the isolated plasmid DNA of transformants was analyzed by sequencing.

Wild-type RNase A and the disulfide variants were produced and purified by methods described previously [10,12], with the following modifications. The inclusion body pellet was resuspended in solubilization buffer (12 mL), which was 20 mM Tris/HCl buffer (pH 8.0) containing guanidine-HCl (7 M), dithiothreitol (0.10 M), and EDTA (10 mM), and shaken at room temperature for 3 h. The reduced protein solution was diluted 10-fold with 20 mM acetic acid and centrifuged for 30 min at 15 300 ***g***. The supernatant was dialyzed exhaustively against 20 mM acetic acid. The soluble fraction was added to folding buffer (1.00 L), which was 0.10 M Tris/acetic acid buffer (pH 8.5) containing NaCl (0.10 M), reduced glutathione (1.0 mM), and oxidized glutathione (0.2 mM), and was stirred gently at 4 °C for 48 h. The purity of the protein after gel filtration and cation-exchange chromatography was assessed by SDS/PAGE and by its A_{280}/A_{260} ratio. Removing a disulfide bond is expected to alter the extinction coefficient of RNase A by $< 1\%$ [13,14]. Hence, concentrations of wild-type RNase A and the disulfide variants were determined by using $\varepsilon = 0.72\ mL \cdot mg^{-1} \cdot cm^{-1}$ at 277.5 nm [15].

Thermal unfolding monitored by ultraviolet spectroscopy

UV spectroscopy was used to determine the effect of replacing a cystine with a pair of alanine residues on the thermal stability of RNase A. As RNase A is unfolded, its six tyrosine residues become exposed to solvent and its molar absorptivity at 287 nm decreases significantly [16]. The thermal stabilities of RNase A and the disulfide variants were assessed by monitoring the change in absorbance at 287 nm with temperature [17,18]. Solutions of protein were dialyzed exhaustively at 4 °C in

30 mM sodium acetate buffer (pH 6.0) containing NaCl (0.10 M). The pH of the acetate buffer does not change significantly (less than 0.3 pH units) over the temperature used in the experiment. The perturbation of T_m within this pH range is minimal [19]. Thermal unfolding curves were obtained as follows. A buffer vs. buffer blank was performed in matched cuvettes at 287 nm at the initial temperature. The absorbance of protein (1.6 mL of a 0.10–0.15 mg·mL^{-1} solution) vs. a buffer blank at 287 nm was recorded at the initial temperature (5 °C) after an 8-min temperature equilibration. As the temperature was increased (from 5 °C to 80 °C in 1 °C increments), absorbance at 287 nm was recorded after an 8-min equilibration at each temperature. As the temperature was decreased from 80 °C to 5 °C in 1 °C increments, the absorbance at 287 nm was recorded after a 5-min equilibration at each temperature.

Thermal unfolding monitored by differential scanning calorimetry

DSC was used to verify the results obtained from UV spectroscopy by monitoring the heat absorbed during the unfolding of wild-type RNase A and the disulfide variants. To prepare samples for DSC, wild-type RNase A and the variants were dialyzed exhaustively against 30 mM sodium acetate buffer (pH 6.0) containing NaCl (0.10 M). Protein solutions and a sample of the final dialysis buffer were centrifuged at 15 300 ***g*** for 30 min to remove particulates. The supernatants were degassed under vacuum, and their protein concentrations (0.64–2.54 mg·mL^{-1}) were determined immediately prior to loading the DSC sample cell. Calorimetric measurements were made on samples under N_2(g) (30 p.s.i.) at a scan rate of 1.0 °C·min^{-1}. The dialysis buffer was used to perform a buffer vs. buffer baseline scan and as the blank in the protein vs. buffer scan. A single transition was observed in each DSC thermogram, and each scan was terminated approximately 20 °C beyond the transition. The unfolding of wild-type RNase A and all four of the disulfide variants was > 99% reversible, as demonstrated by reheating protein samples (data not shown). Data were collected with the program ORIGIN (MicroCal Software; Northampton, MA, USA). Buffer vs. buffer baseline data were subtracted from protein vs. buffer data. Molar heat capacity was obtained by dividing this subtracted quantity by the number of moles of protein in the sample cell.

Steady-state kinetic analyses

The ability of RNase A and the disulfide variants to catalyze the cleavage of poly(C) was assessed using UV spectroscopy. Concentrations of mononucleotide units in poly(C) were determined by UV absorption in 10 mM Tris/HCl buffer (pH 7.8) containing EDTA (1.0 mM) by assuming that $\varepsilon = 6200$ M^{-1}·cm^{-1} at 268 nm [18]. The difference in molar absorptivity between a mononucleotide unit in the polynucleotide substrate and the mononucleotide 2′,3′-cyclic phosphate product was assumed to be $\varepsilon = 2380$ M^{-1}·cm^{-1} at 250 nm [10]. All assays were performed at 10 °C in 0.10 M Mes/NaOH buffer (pH 6.0) containing NaCl (0.10 M), poly(C) (1.18 μM − 2.7 mM), and an appropriate amount of enzyme. Values of k_{cat}, K_m, and k_{cat}/K_m were determined from the initial velocity data with the program HYPERO [20].

RESULTS

Protein production and purification

An *E. coli* T7 RNA polymerase system was used to direct the expression of wild-type RNase A and the disulfide variants [10]. The target proteins accumulated as inclusion bodies, and were folded and purified by using both gel filtration and cation exchange chromatography. After purification, each protein was determined to be > 99% pure by SDS/PAGE. In addition, each protein had $A_{280}/A_{260} > 1.8$, indicating that the preparations were not contaminated significantly with nucleic acid [21]. Approximately 40 mg of pure wild-type RNase A were obtained per L of culture. Following expression of appropriately mutated cDNA in *E. coli* strain BL21(DE3), similar yields were obtained of the C65A/C72A, C40A/C95A and C26A/C84A variants. The C58A/C110A variant was more difficult to fold correctly, yielding only 5 mg of pure protein per L of culture.

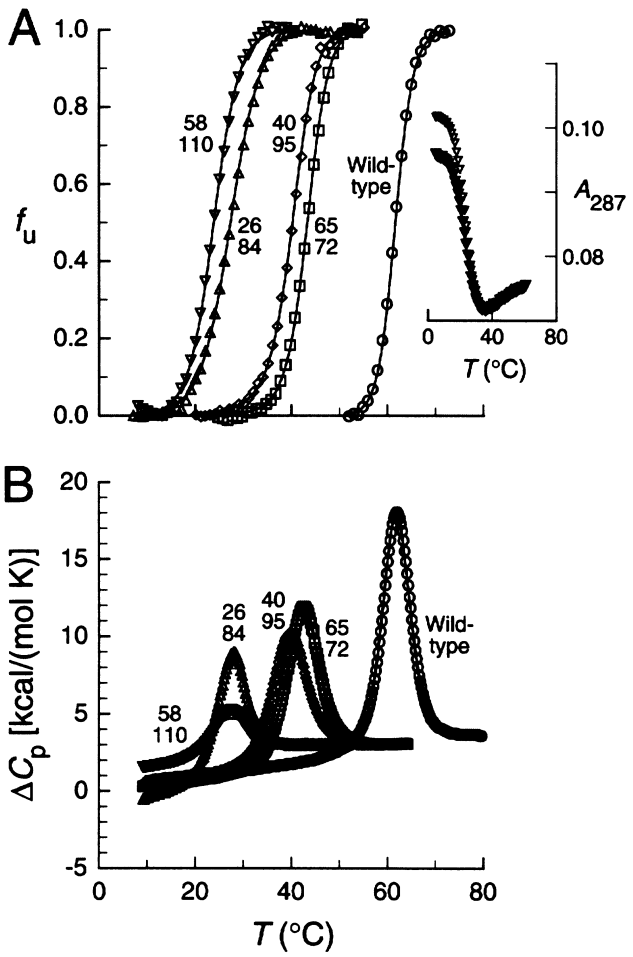

Fig. 2. Unfolding of wild-type ribonuclease A and disulfide variants as monitored by (A) ultraviolet spectroscopy and (B) differential scanning calorimetry. Data are for wild-type RNase A (○), and the C65A/C72A (□), C40A/C95A (◇), C26A/C84A (△), and C58A/C110A (▽) variants in 0.030 M sodium acetate buffer (pH 6.0) containing NaCl (0.10 M). Inset in (A) shows raw data for the thermal denaturation (▽) and renaturation (▼) of C58A/C110A RNase A. Data in (B) have been shifted along the ordinate to equalize the value of C_p for each unfolded protein.

Thermal unfolding monitored by ultraviolet spectroscopy

A plot of A_{287} vs. temperature was converted into one of f_u vs. temperature, where f_u is the fraction of unfolded protein at a given temperature [17]. The reversible thermal unfolding curves of wild-type RNase A and the C65A/C72A, C40A/C95A, C26A/C84A, and C58A/C110A variants are shown in Fig. 2A. The thermal transition of each of the disulfide variants occurred at a lower temperature than did that of wild-type RNase A. The Cys65–Cys72 and Cys40–Cys95 disulfide bonds crosslink surface loops in RNase A. The absence of either disulfide bond destabilizes the protein significantly. In wild-type RNase A, the disulfide bonds between Cys26–Cys84 and Cys58–Cys110 link an α-helix to a β-sheet. The conformational stability of C26A/C84A RNase A or C58A/C110A RNase A is still lower than that of the C65A/C72A or C40A/C95A variant. The absence of either cystine lowers stability such that the C26A/C84A and C58A/C110A variants are approximately half folded at room temperature.

The disulfide bond contribution to conformational stability was determined by fitting the f_u vs. temperature data for wild-type RNase A and the disulfide variants using the program SIGMAPLOT 4.16 (Jandel Scientific; SanRafael, CA) to the equations [17]:

$$\Delta G(T) = (1 - T/T_m) + \Delta C_p[T - T_m - T \ln(T/T_m)] \quad (1)$$

$$\Delta G(T) = -RT \ln K = -RT \ln[f_u/(1 - f_u)] \quad (2)$$

where the subscript '*m*' refers to values at the midpoint of the thermal unfolding curve and $\Delta C_p = 1.15$ kcal·mol^{-1}·K^{-1}) for wild-type RNase A [22] and the disulfide variants. As listed in Table 1, the value of T_m^{UV} (where the superscript *UV* refers to parameters obtained by UV spectroscopy) for the wild-type protein is consistent with values published previously [18,23,24]. The values of T_m^{UV} for C65A/C72A RNase A and C40A/C95A RNase A are decreased by 19.3 °C and 21.2 °C, respectively. Absolute values of T_m^{UV} could not be compared to literature values because of differing solution conditions. Still, the value of ΔT_m^{UV} for C40A/C95A RNase A is similar to a value determined previously [25]. Also, replacing Cys65 and Cys72 with a pair of serine residues results in a value of ΔT_m^{UV} that is similar to that for C65A/C72A RNase A [6]. The values of T_m^{UV} for C26A/C84A RNase A and C58A/C110A RNase A are decreased by 34.4 °C and 37.7 °C, respectively. Replacing Cys26 and Cys84 or Cys58 and Cys110 with a pair of serine residues results in variants that are too unstable to allow for the determination of T_m^{UV} values [6]. The removal of each crosslink caused a large perturbation to the protein and therefore the free energy of perturbation could not be determined for the disulfide variants [26].

Thermal unfolding monitored by differential scanning calorimetry

Solution conditions used during DSC experiments were identical to those used during UV spectroscopic studies. The reversible DSC profiles of the relative heat capacity are shown in Fig. 2B. These profiles were fitted to equations describing a two-state model for unfolding: N⇄U where N is the native state and U is the unfolded state. The change in heat capacity (ΔC_p) upon unfolding has traditionally been assumed to be constant with temperature. Privalov and coworkers have shown that ΔC_p may only be constant over a narrow temperature range and can vary greatly over a broad range of temperature [27]. Our experiments were performed over a broad range of temperature. To model the temperature-dependence in heat capacity, we employed the methods of Privalov and coworkers [28]. Curve fitting was done by nonlinear regression analysis using the program NLREG (P. H. Sherrod, unpublished results). As is apparent from Fig. 2B, the thermal unfolding of wild-type RNase A, C65A/C72A RNase A, and C40A/C95A RNase A fit well to the two-state model. The thermal transition of C26A/C84A RNase A and C58A/C110A RNase A begin below 15 °C and fit less well to the two-state model. Attempts to fit the data to a cold denaturation model were unsuccessful.

Table 1. Thermodynamic parameters for the unfolding of wild-type ribonuclease A and the C65A/C72A, C40A/C95A, C26A/C84A, and C58A/C110A variants. Values were obtained by ultraviolet spectroscopy and differential scanning calorimetry. Values (± SE) from ultraviolet spectroscopy are for triplicate experiments in 0.030 M sodium acetate buffer (pH 6.0) containing NaCl (0.10 M). Values of SE are the standard errors from replicate experiments. Values (± SE) from differential scanning calorimetry are for duplicate experiments performed in 0.030 M sodium acetate buffer (pH 6.0) containing NaCl (0.10 M). Values of SE are the standard errors from replicate experiments. Determinate errors for T_m^{DSC} and ΔH_m^{DSC} are approximately 1% and 5%, respectively.

Ribonuclease A	T_m^{UV} (°C)	T_m^{DSC}	ΔH_m^{DSC} (kcal·mol^{-1})	$\Delta H_{vH}/\Delta H_{cal}$
Wild-type	61.6 ± 0.3	62.1 ± 0.2	113.7 ± 2.8	1.00
C65A/C72A	42.3 ± 0.2	42.7 ± 0.1	91.8 ± 3.3	0.98
C40A/C95A	40.4 ± 0.2	39.3 ± 1.0	77.3 ± 2.1	0.97
C26A/C84A	27.2 ± 1.7	26.8 ± 0.9	70.2 ± 2.5	0.96
C58A/C110A	23.9 ± 0.2	26.1 ± 0.3	45.5 ± 0.7	1.05

Compared to wild-type RNase A, the values of T_m^{DSC} (where the superscript 'DSC' refers to parameters obtained by DSC) for the C65A/C72A, C40A/C95A, C26A/C84A, and C58A/C110A variants are decreased by 19.4, 22.8, 35.3, and 36.0 °C, respectively (Table 1). The values of ΔH_m^{DSC} for the variants are less than that for the wild-type protein. Moreover, as the T_m^{DSC} of a variant decreases, the value of ΔH_m^{DSC} decreases. The values of ΔH_m^{DSC} for wild-type RNase A and the C65A/C72A, C40A/C95A, C26A/C84A and C58A/C110A variants are 113.7, 91.8, 77.3, 70.2, and 45.5 kcal·mol^{-1}, respectively.

The values of van't Hoff enthalpy (ΔH_{vH}) for the unfolding of the wild-type and variant proteins were calculated from the shapes of the calorimetric scans with the equation [29,30]:

$$\Delta H_{vH} = \frac{4RT_m^2}{\Delta H_{cal}}\left(< C_p >_{max} - \frac{\Delta C_p}{2}\right) \quad (3)$$

where $< C_p >_{max}$ is the heat capacity at the T_m^{DSC} and the calorimetric enthalpy (ΔH_{cal}) is equal to the area under the DSC curve (Fig. 2B). A van't Hoff enthalpy equal to the calorimetric enthalpy is evidence of two-state unfolding [30]. As listed in Table 1, the values of $\Delta H_{vH}/\Delta H_{cal}$ for wild-type RNase A and the C65A/C72A, C40A/C95A, C26A/C84A, and C58A/C110A variants are 1.00, 0.98, 0.97, 0.96, and 1.05, respectively.

Steady-state kinetic parameters

Wild-type RNase A enhances the rate of RNA cleavage by 10^{12}-fold compared to the uncatalyzed reaction [31]. All four disulfide variants are also efficient catalysts of RNA cleavage. This efficiency is consistent with each disulfide variant being folded correctly and having a three-dimensional structure

Table 2. Steady-State kinetic parameters for catalysis by wild-type ribonuclease A and the C65A/C72A, C40A/C95A, C26A/C84A, and C58A/C110A variants. Assays were performed at 10 °C in 0.10 M Mes/NaOH buffer (pH 6.0) containing NaCl (0.10 M). Values (± SE) of K_m and k_{cat}/K_m are based on nucleotide units in poly(cytidylic acid).

Ribonuclease A	k_{cat} (s^{-1})	K_m (mM)	k_{cat}/K_m (10^6 $M^{-1}\cdot s^{-1}$)
Wild-type	190 ± 11	0.047 ± 0.011	4.0 ± 1.0
C65A/C72A	43 ± 5	0.42 ± 0.13	0.10 ± 0.03
C40A/C95A	44 ± 3	0.34 ± 0.07	0.13 ± 0.03
C26A/C84A	135 ± 20	0.19 ± 0.07	0.71 ± 0.28
C58A/C110A	147 ± 3	0.084 ± 0.007	1.76 ± 0.15

similar to that of wild-type RNase A. Wild-type RNase A and the disulfide variants all begin their thermal unfolding transitions above 13 °C (Fig. 2). Steady-state kinetic parameters for the cleavage of poly(C) by wild-type RNase A and the disulfide variants were therefore determined at 10 °C, where all proteins are > 99% folded. The values of these parameters are listed in Table 2.

The replacement of a cystine with a pair of alanine residues decreases the value of k_{cat} (Table 2). C58A/C110A RNase A and C26A/C84A RNase A have a 1.3- to 1.4-fold lower k_{cat} than does the wild-type enzyme. The value of k_{cat} is affected more significantly for C40A/C95A RNase A and C65A/C72A RNase A (4.3- to 4.4-fold). A moderate (1.8- to 8.9-fold) increase in the value of K_m is apparent for each disulfide variant relative to that of wild-type RNase A. Furthermore, the values of K_m for the C65A/C72A and C40A/C95A variants are increased to a greater extent than are those for the C58A/C110A and C26A/C84A variants. The values of k_{cat}/K_m for the RNase A disulfide variants are 2.3- to 40-fold lower than that of the wild-type enzyme (Table 2).

DISCUSSION

The stability of RNase A is legendary. For example, the classical procedure for the purification of RNase A from a bovine pancreas relies on the enzyme maintaining its integrity and solubility under harsh conditions: first, 0.25 N sulfuric acid at 5 °C, and then, pH 3.0 at 95–100 °C [32]. These conditions disrupt noncovalent interactions but do not break the four disulfide bonds of RNase A, which are disposed in an interweaving but symmetrical network that crosslinks various elements of its secondary structure (Fig. 1).

Disulfide bond-mediated contributions to conformational stability

Disulfide bonds are the only common covalent crosslinks in polypeptide chains. Crosslinks limit the number of unfolded conformations of a polypeptide chain, thereby destabilizing the unfolded state relative to the native state [33]. If this loss of entropy in the unfolded state were the only disulfide bond-mediated contribution to conformational stability, then disulfide bond-mediated stability would be reflected in the loop size, i.e. the number of amino-acid residues (η) within the ring containing the disulfide bond [33]. This model has also been applied to proteins with interweaving crosslinks, including RNase A [34,35]. A disulfide bond within a large ring would decrease the stability of the unfolded state more than one within a small ring. Introduction of a new disulfide bond into a protein structure can either increase [36–39] or decrease [40–42] conformational stability.

To dissect the contributions of disulfide bonds to the conformational stability and catalytic activity of RNase A, we chose to replace each cystine with a pair of alanine residues, which is the most conservative natural replacement for a cystine. Each cystine side chain of RNase A has a solvent-accessible surface area of < 0.07 nm^2 (Fig. 1), which is < 15% of the maximum. Replacing a buried cystine in BPTI with an alanine residue and a serine residue or with two serine residues was found to be more destabilizing than replacing it with a pair of alanine residues [43]. Likewise, the results of molecular dynamics simulations suggest that replacing a cysteine residue in the core of BPTI with serine is more unfavorable than is replacing it with alanine [44,45].

The thermal unfolding of wild-type RNase A and each of the four disulfide variants were monitored by UV spectroscopy and DSC. These two methods probe different aspects of protein unfolding. UV spectroscopy reports on the change in molar absorptivity as the protein unfolds. DSC reports directly on the heat absorbed during protein unfolding. The values of T_m obtained by these two distinct methods are in gratifying agreement (Table 1), and show that each disulfide bond of RNase A contributes significantly to its thermal stability.

The relative contribution of each disulfide bond to the conformational stability of RNase A depends on its location within the polypeptide chain relative to the other disulfide bonds. This disulfide bond connectivity is shown in Fig. 1. Disulfide bonds that tether otherwise free residues of a polypeptide chain are likely to decrease the conformational entropy of the unfolded state (and thus enhance conformational stability) more than disulfide bonds that crosslink residues that are otherwise restrained [8,46]. Of the four RNase A disulfide bonds, Cys26–Cys84 and Cys58–Cys110 contribute most significantly to conformational stability (Table 1). These disulfide bonds are the outermost crosslinks in the polypeptide chain. When the Cys26–Cys84 disulfide bond is removed, 14 N-terminal residues become less restricted. Likewise, when the Cys58–Cys110 disulfide bond is removed, 15 C-terminal residues are liberated.

The Cys40–Cys95 disulfide bond encloses a loop of similar size to that of the Cys26–Cys84 and Cys58–Cys110 disulfide bonds (Fig. 1). Yet, the Cys40–Cys95 disulfide bond contributes less to conformational stability (Table 1). Residues 40–95 are constrained by three overlapping disulfide bonds: Cys26–Cys84, Cys40–Cys95, and Cys58–Cys110. Even in the absence of the Cys40–Cys95 disulfide bond, residues 40–95 are restricted by the two more terminal crosslinks.

Of the four disulfide bonds in RNase A, the Cys65–Cys72 disulfide bond encloses the smallest loop and contributes the least to conformational stability. Interestingly, the Cys65–Cys72 disulfide bond is the only disulfide bond that is not absolutely conserved throughout the ribonuclease A superfamily [5]. For example, this disulfide bond is absent from the RNase A homologs in snapping turtle [47] and iguana [48] as well as from the angiogenins [49,50] and Onconase™ [51]. The ribonucleolytic activity of each of these enzymes is less than that of RNase A [48,52–55], as expected from our analysis of catalysis by the C65A/C72A variant (see below).

Disulfide bond-mediated contributions to catalytic activity

Disulfide bonds can be important for the function of a protein, as well as its conformational stability. Indeed, replacing a

native disulfide bond with a pair of alanine residues can result in a variant protein that has greater conformational stability than does the wild-type protein [56]. In other words, a native disulfide bond can actually destabilize the tertiary structure. Such disulfide bonds may be retained by natural selection to enable a particular function [57,58].

RNase A catalyzes the cleavage of the P-$O^{5'}$ bond of RNA on the 3′ side of pyrimidine residues to yield a 2′,3′-cyclic phosphodiester. His12 and His119 are the base and acid that mediate the transphosphorylation reaction [59]. Lys41 assists in transition state stabilization [60]. Replacing any of these three residues with alanine hinders catalysis by 10^4- to 10^5-fold [4]. To achieve the maximal rate of substrate cleavage, each active-site residue must be aligned precisely.

The steady-state kinetic parameters for catalysis by the disulfide variants are similar to those of the wild-type enzyme. Yet for each variant enzyme, the value of K_m is increased and the value of k_{cat} is decreased (Table 2). Apparently, each disulfide bond serves to orient more precisely the active-site residues.

The disulfide bonds that are least important to conformational stability are most important to catalytic activity. The loss of a disulfide bond near the active site (Cys65–Cys72 and Cys40–Cys95; Fig. 1) affects catalysis more dramatically than does the loss of a more remote disulfide bond (Cys26–Cys84 and Cys58–Cys110). The Cys65–Cys72 and Cys40–Cys95 disulfide bonds contribute 40-and 31-fold, respectively, to k_{cat}/K_m, whereas the Cys26–Cys84 and Cys58–Cys110 disulfide bonds contribute only 6-and 2-fold, respectively (Table 2).

The Cys65–Cys72 and Cys40–Cys95 disulfide bonds are proximal to key enzymic residues. The half-cystine at residue 40 is adjacent to Lys41. Removing a hydrogen bond to the main-chain oxygen of Lys41 diminishes catalytic activity [18]. In the C40A/C95A variant, large localized perturbations disrupt the orientation of Lys41 [25]. Likewise, without the Cys65–Cys72 disulfide bond, the 65–72 surface loop is more flexible [61]. The half-cystine at residue 65 is adjacent to Lys66. The main chain of Lys66 assists in aligning His119 [62]. Moreover, a Coulombic interaction between the side chain of Lys66 and an RNA substrate is important for catalysis [63]. Thus, the Cys65–Cys72 and Cys40–Cys95 disulfide bonds may have evolved, at least in part, to position precisely residues important for catalysis of RNA cleavage.

ACKNOWLEDGEMENTS

We thank Drs Darrell R. McCaslin and L. Wayne Schultz for assistance. This work was supported by grants GM44783 (National Institutes of Health) and BES-9604563 (National Science Foundation). T. A. K. was supported by an Advanced Opportunity Fellowship. K. J. W. was supported by a WARF predoctoral fellowship and Chemistry–Biology Interface Training Grant GM08505 (NIH). K. M. T. was supported by a Howard Hughes Medical Institute predoctoral fellowship. Calorimetry data were obtained at the University of Wisconsin–Madison Biophysical Instrumentation Facility, which was supported by the University of Wisconsin–Madison and grant BIR-9512577 (NSF).

REFERENCES

1. Anfinsen, C.B. (1973) Principles that govern the folding of protein chains. *Science* **181**, 223–230.
2. Dill, K.A. (1990) Dominant forces in protein folding. *Biochemistry* **29**, 7133–7155.
3. D'Alessio, G. & Riordan, J.F., eds. (1997). *Ribonucleases: Structures and Functions*. Academic Press, New York.
4. Raines, R.T. (1998) Ribonuclease A. *Chem. Rev.* **98**, 1045–1065.
5. Beintema, J.J., Schüller, C., Irie, M. & Carsana, A. (1988) Molecular evolution of the ribonuclease superfamily. *Prog. Biophys. Mol. Biol.* **51**, 165–192.
6. Laity, J.H., Shimotakahara, S. & Scheraga, H.A. (1993) Expression of wild-type and mutant bovine pancreatic ribonuclease A in *Escherichia coli*. *Proc. Natl Acad. Sci. USA* **90**, 615–619.
7. Chothia, C. (1976) The nature of the accessible and buried surfaces in proteins. *J. Mol. Biol.* **105**, 1–14.
8. Thornton, J.M. (1981) Disulfide bridges in globular proteins. *J. Mol. Biol.* **151**, 261–287.
9. Saunders, A.J., Young, G.B. & Pielak, G.J. (1993) Polarity of disulfide bonds. *Protein Sci.* **2**, 1183–1184.
10. delCardayré, S.B., Ribó, M., Yokel, E.M., Quirk, D.J., Rutter, W.J. & Raines, R.T. (1995) Engineering ribonuclease A: production, purification, and characterization of wild-type enzyme and mutants at Gln11. *Protein Eng.* **8**, 261–273.
11. Kunkel, T.A., Roberts, J.D. & Zakour, R.A. (1987) Rapid and efficient site-specific mutagenesis without phenotypic selection. *Methods Enzymol.* **154**, 367–382.
12. Kim, J.-S. & Raines, R.T. (1993) Bovine seminal ribonuclease produced from a synthetic gene. *J. Biol. Chem.* **268**, 17392–17396.
13. Gill, S.C. & von Hippel, P.H. (1989) Calculation of protein extinction coefficients from amino acid sequence data. *Anal. Biochem.* **182**, 319–326.
14. Pace, C.N., Vajdos, F., Fee, L., Grimsley, G. & Gray, T. (1995) How to measure and predict the molar absorption coefficient of a protein. *Protein Sci.* **4**, 2411–2423.
15. Sela, M., Anfinsen, C.B. & Harrington, W.F. (1957) The correlation of ribonuclease activity with specific aspects of tertiary structure. *Biochim. Biophys. Acta* **26**, 502–512.
16. Hermans, J.J. & Scheraga, H.A. (1961) Structural studies of ribonuclease. V. Reversible change of configuration. *J. Am. Chem. Soc.* **83**, 3283–3292.
17. Pace, C.N., Shirley, B.A. & Thomson, J.A. (1989) Measuring the conformational stability of a protein. In *Protein Structure* (Creighton, T.E., ed.), pp. 311–330. IRL Press, New York.
18. Eberhardt, E.S., Wittmayer, P.K., Templer, B.M. & Raines, R.T. (1996) Contribution of a tyrosine side chain to ribonuclease A catalysis and stability. *Protein Sci.* **5**, 1697–1703.
19. Quirk, D.J., Park, C., Thompson, J.E. & Raines, R.T. (1998) His···Asp catalytic dyad of ribonuclease A: conformational stability of the wild-type, D121N, D121A, and H119A enzymes. *Biochemistry* **37**, 17958–17964.
20. Cleland, W.W. (1979) Statistical analysis of enzyme kinetic data. *Methods Enzymol.* **63**, 103–138.
21. Layne, E. (1957) Spectrophotometric and turbidimetric methods for measuring proteins. *Methods Enzymol.* **3**, 447–454.
22. Pace, C.N., Grimsley, G.R., Thomas, S.T. & Makhatadze, G.I. (1999) Heat capacity change for ribonuclease A folding. *Protein Sci.* **8**, 1500–1504.
23. Santoro, M.M., Liu, Y., Khan, S.M.A., Hou, L.-X. & Bolen, D.W. (1992) Increased thermal stability of proteins in the presence of naturally occurring osmolytes. *Biochemistry* **31**, 5278–5283.
24. Catanzano, F., Graziano, G., Cafaro, V., D'Alessio, G., Donato, A.D. & Barone, G. (1997) From ribonuclease A toward bovine seminal ribonuclease: a step by step thermodynamic analysis. *Biochemistry* **36**, 14403–14408.
25. Laity, J.H., Lester, C.C., Shimotakahara, S., Zimmerman, D.E., Montelione, G.T. & Scheraga, H.A. (1997) Structural characterization of an analog of the major rate-determining disulfide folding intermediate of bovine pancreatic ribonuclease A. *Biochemistry* **36**, 12683–12699.
26. Becktel, W.J. & Schellman, J.A. (1987) Protein stability curves. *Biopolymers* **26**, 1859–1877.
27. Wintrode, P.L., Makhatadze, G.I. & Privalov, P.L. (1994) Thermodynamics of ubiquitin unfolding. *Proteins* **18**, 246–253.
28. Privalov, P.L., Tiktopulo, E.I., Venyaminov, S.Y., Griko, Y.V., Makhatadze, G.I. & Khechinashvili, N.N. (1989) Heat capacity and

conformation of proteins in the denatured state. *J. Mol. Biol.* **205**, 737–750.
29. Privalov, P.L. & Potekhin, S.A. (1986) Scanning microcalorimetry in studying temperature-induced changes in proteins. *Adv. Enzymol.* **131**, 4–51.
30. Carra, J.H., Murphy, E.C. & Privalov, P.L. (1996) Thermodynamic effects of mutations on the denturation of T4 lysozyme. *Biophys. J.* **71**, 1994–2001.
31. Thompson, J.E., Kutateladze, T.G., Schuster, M.C., Venegas, F.D., Messmore, J.M. & Raines, R.T. (1995) Limits to catalysis by ribonuclease A. *Bioorg. Chem.* **23**, 471–481.
32. Kunitz, M. & McDonald, M.R. (1953) Ribonuclease. *Biochem. Prep.* **3**, 9–19.
33. Flory, P.J. (1956) Theory of elastic mechanisms in fibrous proteins. *J. Am. Chem. Soc.* **78**, 5222–5235.
34. Poland, D.C. & Scheraga, H.A. (1965) Statistical mechanics of noncovalent bonds in polyamino acids. VIII. Covalent loops in proteins. *Biopolymers* **3**, 379–399.
35. Pace, C.N., Grimsley, G.R., Thomson, J.A. & Barnett, B.J. (1988) Conformational stability and activity of ribonuclease T1 with zero, one, and two intact disulfide bonds. *J. Biol. Chem.* **263**, 11820–11825.
36. Villafranca, J.E., Howell, E.E., Oatley, S.J., Xuong, N.-H. & Kraut, J. (1987) An engineered disulfide bond in dihydrofolate reductase. *Biochemistry* **26**, 2182–2189.
37. Matsumura, M., Signor, G. & Matthews, B.W. (1989) Substantial increase of protein stability by multiple disulphide bonds. *Nature* **342**, 291–293.
38. Ko, J.H., Jang, W.H., Kim, E.K., Lee, H.B., Park, K.D., Chung, J.H. & Yoo, O.J. (1996) Enhancement of thermostability and catalytic efficiency of AprP, and alkaline protease from *Pseudomonas* sp., by introduction of a disulfide bond. *Biochem. Biophys. Res. Commun.* **221**, 631–635.
39. Yamaguchi, S., Takeuchi, K., Mase, T., Oikawa, K., McMullen, T., Derewenda, U., McElhaney, R.N., Kay, C.M. & Derewenda, Z.S. (1996) The consequences of engineering an extra disulfide bond in the *Penicillium camembertii* mono- and diglyceride specific lipase. *Protein Eng.* **9**, 789–795.
40. Wells, J.A. & Powers, D.B. (1986) *In vivo* formation and stability of engineered disulfide bonds in subtilisin. *J. Biol. Chem.* **261**, 6564–6570.
41. Matsumura, M., Becktel, W.J., Levitt, M. & Matthews, B.W. (1989) Stabilization of phage T4 lysozyme by engineered disulfide bonds. *Proc. Natl Acad. Sci. USA* **86**, 6562–6566.
42. Betz, S.F., Marmorion, J.L., Saunders, A.J., Doyle, D.F., Young, G.B. & Pielak, G.J. (1996) Unusual effects of an engineered disulfide on global and local protein stability. *Biochemistry* **35**, 7422–7428.
43. Lui, Y., Breslauer, K. & Anderson, S. (1997) 'Designing out' disulfide bonds: thermodynamic properties of 30–51 cystine substitution mutants of bovine trypsin inhibitor. *Biochemistry* **36**, 5323–5335.
44. Darby, N.J., van Mierlo, C.P. & Creighton, T.E. (1991) The [5–55] single-disulphide intermediate in folding of bovine pancreatic trypsin inhibitor. *FEBS Lett.* **279**, 61–64.
45. Staley, J.P. & Kim, P.S. (1992) Complete folding of bovine pancreatic trypsin inhibitor with only a single disulfide bond. *Proc. Natl Acad. Sci. USA* **89**, 1519–1523.
46. Harrison, P.M. & Sternberg, M.J.E. (1994) Analysis and classification of disulphide connectivity in proteins – the entropic effect of cross-linkage. *J. Mol. Biol.* **244**, 448–463.
47. Beintema, J.J. & van der Laan, J.M. (1986) Comparison of the structure of turtle pancreatic ribonuclease with those of mammalian ribonucleases. *FEBS Lett.* **194**, 338–342.
48. Zhao, W., Beintema, J.J. & Hofsteenge, J. (1994) The amino acid sequence of iguana (*Iguana iguana*) pancreatic ribonuclease. *Eur. J. Biochem.* **219**, 641–646.
49. Strydom, D.J., Fett, J.W., Lobb, R.R., Alderman, E.M., Bethune, J.L., Riordan, J.F., Vallee, B. & l. (1985) Amino acid sequence of human tumor derived angiogenin. *Biochemistry* **24**, 5486–5494.
50. Bond, M.D., Strydom, D.J. & Vallee, B.L. (1993) Characterization and sequencing of rabbit, pig and mouse angiogenins: discernment of functionally important residues and regions. *Biochim. Biophys. Acta* **1162**, 177–186.
51. Ardelt, W., Mikulski, S.M. & Shogen, K. (1991) Amino acid sequence of an anti-tumor protein from *Rana pipiens* oocytes and early embryos. *J. Biol. Chem.* **266**, 245–251.
52. Katoh, H., Yoshinaga, M., Yanagita, T., Ohgi, K., Irie, M., Beintema, J.J. & Meinsma, D. (1986) Kinetic studies on turtle pancreatic ribonuclease: a comparative study of the base specificities of the B_2 and P_0 sites of bovine pancreatic ribonuclease A and turtle pancreatic ribonuclease. *Biochim. Biophys. Acta* **873**, 367–371.
53. Boix, E., Wu, Y., Vasandani, V.M., Saxena, S.K., Ardelt, W., Ladner, J. & Youle, R.J. (1996) Role of the N terminus in RNase A homologues: Differences in catalytic activity, ribonuclease inhibitor interaction and cytotoxicity. *J. Mol. Biol.* **257**, 992–1007.
54. Leland, P.A., Schultz, L.W., Kim, B.-M. & Raines, R.T. (1998) Ribonuclease A variants with potent cytotoxic activity. *Proc. Natl Acad. Sci. USA* **98**, 10407–10412.
55. Kelemen, B.R., Klink, T.A., Behlke, M.A., Eubanks, S.R., Leland, P.A. & Raines, R.T. (1999) Hypersensitive substrate for ribonucleases. *Nucleic Acids Res.* **27**, 3696–3701.
56. Zhu, H., Dupureur, C.M., Zhang, X. & Tsai, M.D. (1995) Phospholipase A2 engineering. The roles of disulfide bonds in structure, conformational stability, and catalytic function. *Biochemistry* **34**, 15307–15314.
57. Blake, C.C., Ghosh, M., Harlos, K., Avezoux, A. & Anthony, C. (1994) The active site of methanol dehydrogenase contains a disulphide bridge between adjacent cysteine residues. *Nat. Struct. Biol.* **1**, 102–105.
58. Wang, E.C.W., Hung, S.-H., Cahoon, M. & Hedstrom, L. (1997) The role of the Cys191–Cys220 disulfide bond in trypsin: new targets for engineering substrate specificity. *Protein Eng.* **10**, 405–411.
59. Findlay, D., Herries, D.G., Mathias, A.P., Rabin, B.R. & Ross, C.A. (1961) The active site and mechanism of action of bovine pancreatic ribonuclease. *Nature* **190**, 781–784.
60. Messmore, J.M., Fuchs, D.N. & Raines, R.T. (1995) Ribonuclease A: revealing structure–function relationships with semisynthesis. *J. Am. Chem. Soc.* **117**, 8057–8060.
61. Shimotakahara, S., Ríos, C.B., Laity, J.H., Zimmerman, D.E., Scheraga, H.A. & Montelione, G.T. (1997) NMR structural analysis of an analog of an intermediate formed in the rate-determining step of one pathway in the oxidative folding of bovine pancreatic ribonuclease A: automated analysis of ^{1}H, ^{13}C, and ^{15}N resonance assignments for wild-type and [C65S, C72S] mutant forms. *Biochemistry* **36**, 6915–6929.
62. Schultz, L.W., Quirk, D.J. & Raines, R.T. (1998) His···Asp catalytic dyad of ribonuclease A: structure and function of the wild-type, D121N, and D121A enzymes. *Biochemistry* **37**, 8886–8898.
63. Fisher, B.M., Ha, J.-H. & Raines, R.T. (1998) Coulombic forces in protein–RNA interactions: binding and cleavage by ribonuclease A and variants at Lys7, Arg10, and Lys66. *Biochemistry* **37**, 12121–12132.